KMS Technologies – KJT Enterprises, Inc.

Time Domain Controlled Source Electromagnetics for Hydrocarbon Applications

Strack, K.-M. Hanstein, T., Stoyer, C. H., and Thomsen, L. A.

The Earth's Magnetic Interior
IAGA Special Sopron book series
2011

Time Domain Controlled Source Electromagnetics for Hydrocarbon Applications

7

K.M. Strack, T. Hanstein, C.H. Stoyer, and L.A. Thomsen

Abstract

During the past 10 years, marine electromagnetics has developed from infancy into a sizable geophysical industry. While this is feasible in the time and the frequency domains, most of the commercial marine hydrocarbon applications operate in frequency domain, i.e. Controlled-Source Electromagnetic (fCSEM). Until 5 years ago, it was generally assumed that time domain (tCSEM^{TM}) methods would not be of any use in oil exploration. Since then, however, many such measurements have been recorded with several independent tCSEM^{TM} systems that already exist or under development. Time domain measurements can be used everywhere and more suitable for shallow water. They have large anomalous responses than those in fCSEM. From the physical viewpoint, time domain measurements are complementary to frequency domain measurements, as they focus on different spatial regions. With recent advances in electronics time-domain CSEM data can reliably be acquired in an offshore environment. Multiple surveys using autonomous receiver nodes have successfully acquired marine time domain CSEM data. Our work takes the technology a step further, by developing a high-density marine cabled system with novel 5-component sensor package.

7.1 Introduction

For over 50 years, the seismic method has been the geophysical workhorse of the oil exploration industry. While it offers the best description of reservoir shape and stratigraphy, it falls short in describing the fluid properties of the pore space, since seismic waves respond to *both* rock matrix and fluid components of the rock, which are difficult to separate. Usually, fluid discrimination with seismic waves depends on amplitude analysis, which in turn depends on true-amplitude migration of high-quality seismic data that is not always possible.

In particular, many of the changes that take place during the production life of a reservoir do not exhibit a detectable acoustic property change. Since the CSEM response to thin resistors was understood, marine CSEM methods have found application for direct hydrocarbons detection (Eidesmo et al. 2002). While fCSEM has been studied for many years (Cox 1981, Cox et al. 1986, Sinha et al. 1990, Constable and Cox 1996, Constable 2006), little or no work has been done using time domain in an equivalent mode for hydrocarbon exploration. The use of marine CSEM has now gained momentum, and has become one of the most

K.M. Strack (✉)
KMS Technologies, Houston, TX, USA
e-mail: kurt@kmstechnologies.com

E. Petrovský et al. (eds.), *The Earth's Magnetic Interior*, IAGA Special Sopron Book Series 1,
DOI 10.1007/978-94-007-0323-0_7,

significant technology development in oil exploration, since the advent of 3D seismics. As mentioned earlier, most marine EM applications are in frequency domain, with limited ventures in time domain (Edwards 1987, 1997, Edwards and Yu 1993, Ziolkowski et al. 2006). Time domain measurements in marine environment have usually been restricted to near-surface applications with fixed length towed systems (Edwards et al. 1985, Chave et al. 1991, Cheesman et al. 1987, Edwards 1997), or for deeper hydrocarbon applications in shallow water and induced polarization (Strack and Petrov 2007, Strack et al. 2008, Veeken et al. 2009).

We have selected a time domain (tCSEM^{TM}) version, which employs time variant electromagnetic fields of either natural or artificial origin, causing eddy currents within the conductive sediment layers. Our choice is based on the success of time domain measurements on land and its response to thin resistive layers (Eadie 1979, Passalacqua 1983, Strack 1992, 1999, Strack et al. 1989). Unlike other time domain users (e.g. Holten et al. 2009a, b) that focus strongly on the induced polarization effect, we use a normal moving source system and can even use a standard frequency domain system with an additional source, tow over the receiver spread. The induced eddy currents are time variant as well, and they cause a secondary EM field that can be sensed with magnetic or electric sensors placed on the sea floor or in the wellbore. High resistivity lithologies and pore fluids are the resistors that alter the artificial electric field. Recent theoretical and practical evaluations on this aspect can be found in (Weiss 2007, Davydycheva and Rykhlinski 2009). Both favor time domain measurements although, most service providers of CSEM technology still transmit from a frequency-based source with a continuous sinusoid or a square wave. Our time domain signal uses much larger time (tens of seconds) between current switching, so that each switching constitutes a separate transient source. We record the Earth's transient response, while the current is off. We call this tCSEM^{TM}.

7.2 Background Physics

The theory of time-varying electromagnetic fields in a stratified Earth is described in a comprehensive fashion by Ward and Hohmann (1988) and for continuous and transient soundings by Kaufman and Keller (1983) with summaries for grounded dipoles given by Strack (1992, 1999). Responses for various 3D models are described by Hohmann (1988), Newman and Alumbaugh (2000), Druskin and Knizhnerman (1994), Davydycheva et al. (2003).

We follow the standard approach for marine application and fine-tune the digital filters that carry out the Hankel transform for high contrast boundaries. The measured voltages are corrected for frequency dependence of the sensors, processed for signal-to-noise improvement, and then input to the inversion.

With tCSEM^{TM}, one transmits current into the Earth, charging the zones where resistivity varies at the subsurface. The current is then switched "off" and the charge dissipates. Sensors that record the electric and magnetic components measure transient responses to this artificial electric field. Because the time domain method is only measuring the secondary field, it offers a solution to the shallow water limitations that confront frequency-targeted techniques (Weiss 2007 and Avdeeva et al. 2007). The duration of these "on" and "off" times of the source are optimized to each particular problem. Additionally, every current switching represents an initiation time, or time zero, for a given transient. Figure 7.1 shows a typical time domain source waveform and the resulting electric and magnetic fields.

To illustrate the behavior of the electromagnetic field, consider the survey configuration as shown in Fig. 7.2. A dipole source, usually about 300 m long, is

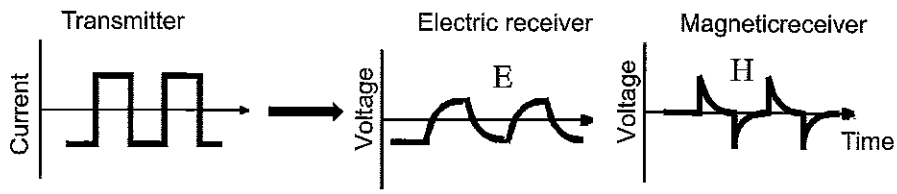

Fig. 7.1 Time domain source waveform and its resulting electric and time derivative of the magnetic fields

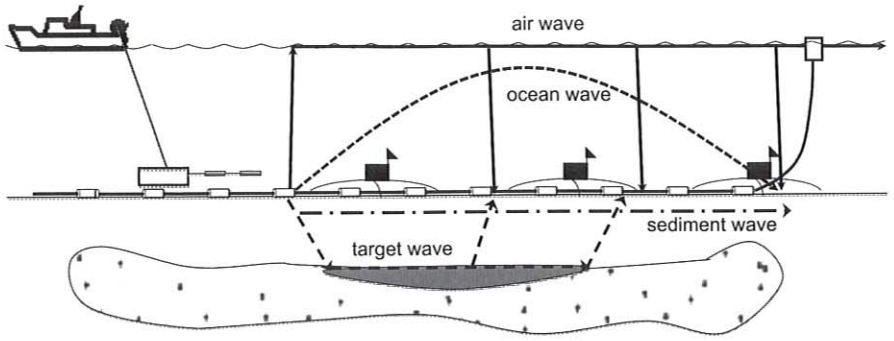

Fig. 7.2 Survey setup for a marine time domain electromagnetic system including nodes and cabled receivers

towed about 30 m above the sea floor. An electric current, as shown in Fig. 7.1, is injected between source electrodes, and the response of this current diffusing into the subsurface is measured with multi-component receivers that are either autonomous (nodes) or connected by a cable. The following wave model as illustrated in Fig. 7.2 can describe the received signal. (Note that more resistive is the path, faster is the propagation speed.)

- Part of the signal travels up to the surface from the transmitter below, then along the air-water interface with speed of light, arrives at the receiver; it is called the air wave.
- Part of the signal goes through the water column, and is called the ocean wave. Traveling through water, the ocean wave arrives later than the airwave and (depending on water depth) sometimes so much delayed that it arrives later than the subsurface response.
- Part of the signal diffuses through the subsurface sediments (usually more resistive than the reservoir) and is called the sediment wave.
- Finally, part of the signal diffuses deep into the subsurface, then refracts along the (resistive) reservoir where it travels faster than the sediment wave; this is called the target wave.
- When the electromagnetic energy diffuses into the medium, its energy (or Pointing vector) travels with similar speed as refracted seismic waves (Weidelt 2007), and we thus call it waves.

To illustrate the different "wave" components, we have calculated the responses and presented in Fig. 7.3. The Earth model is a half space that consists of ocean only; the transmitter and receiver are separated by 1000 m. We simulate the airwave and the ocean wave by placing a transmitter and receiver system close to the sea surface, so that the airwave dominates, and also far away from the air-water interface, so that the ocean wave dominates. The airwave response is shown as a black spike on the ordinate. Because it travels at the speed of light it appears at $t = 0$ on the time scale. The signal with only ocean wave response is the signal that has only one "hump" at approximately 1 s. The curves between these end-members are obtained as the transmitter-receiver and lowered together into the ocean. They exhibit first as airwaves and then ocean waves at later times. As the depth increases, the airwave spreads, due to dispersion in the water on the way up and down. At large depths, the two waves merge. In practice, an impulsive response is realized by time-differentiation of a step response.

We can now display the individual measurements similar to seismic-style traces, as suggested by Edwards (1997) for gas hydrates and by Wright et al. (2002) for land electromagnetic applications. Figures 7.4, 7.5, 7.6, and 7.7 show common-source gathers, where each vertical trace represents a measurement at an offset surface location. The gathers are 500 m apart, starting at 500 m from the transmitter to 10 km maximum offset. Each trace is normalized, to compensate for amplitude attenuation. This seismic-style operation serves much the same purpose as conversion to apparent resistivity. It removes the amplitude effects at far offsets. Of course the normalization factors are retained for later restoration of true amplitudes. On the vertical scale is the diffusion time after switching the transmitter; the scale goes from 0 to 25 s.

Figure 7.4 shows the gather for two of the models used in Fig. 7.3. The top of Fig. 7.4 shows the model

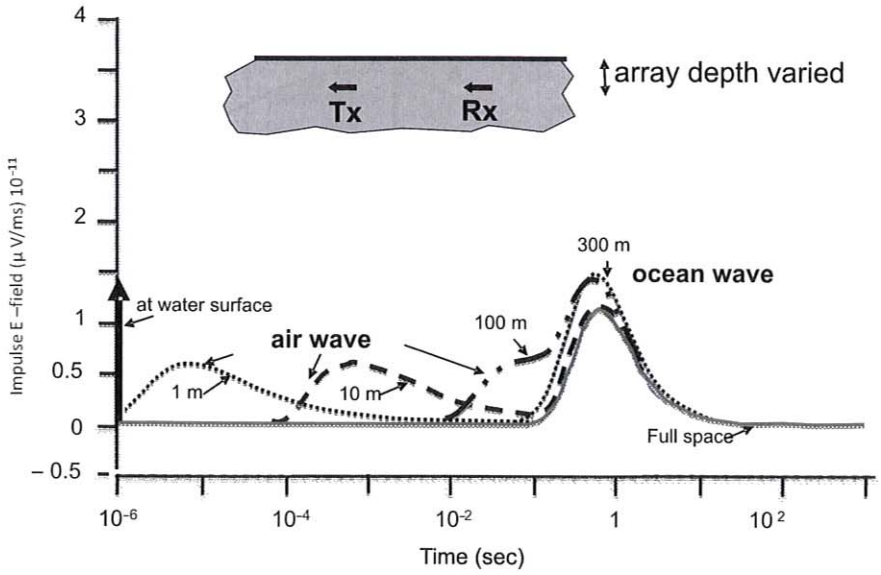

Fig. 7.3 Impulse response for an inline electric field marine CSEM setup for different transmitter-receiver depths below the water surface. The horizontal scale is time in seconds after the impulse

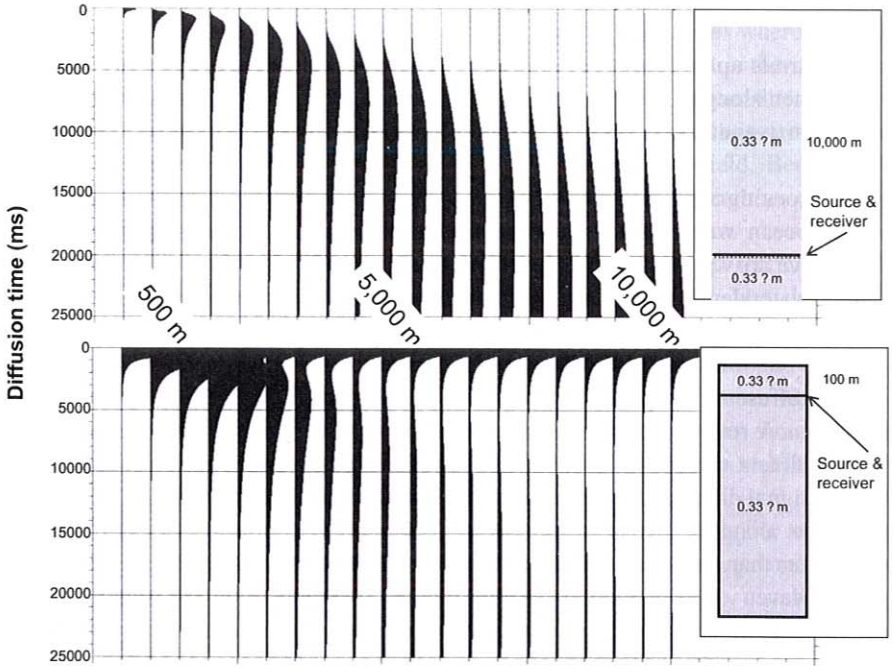

Fig. 7.4 Common-source gathers for impulse response of an inline electric field marine tCSEM setup. The traces represent different offsets between source and receiver; displayed are measured voltages. All traces are displayed trace-normalized. The Earth model is a half space with the resistivity of seawater. The *top* gather represents the case when the system is in deep water and far away from the sea-air interface. The *bottom* gather represents the case when the system is near the air-water interface and includes the airwave (After Allegar et al. 2008)

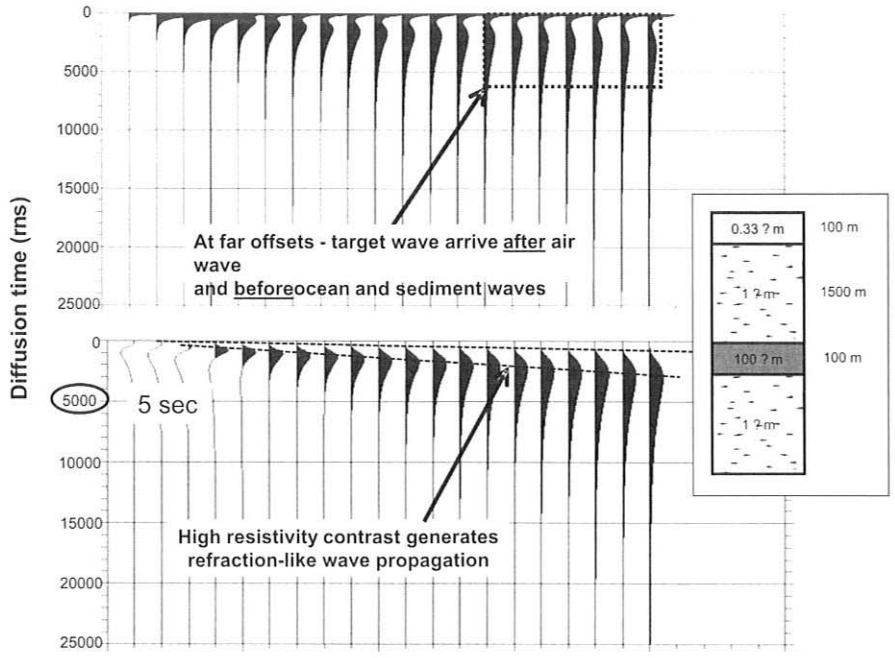

Fig. 7.5 Common-source gathers for the impulse response of an inline electric field marine tCSEM setup. The traces represent different offsets between source and receiver; displayed are measured voltages. All traces are displayed trace-normalized. The Earth model has an oil reservoir at 1500 m depth below the seafloor. The top gather contains all wave components (air wave, ocean wave, sediment wave and target wave). The bottom gather only contains the reservoir response after removal of all other components (After Allegar et al. 2008)

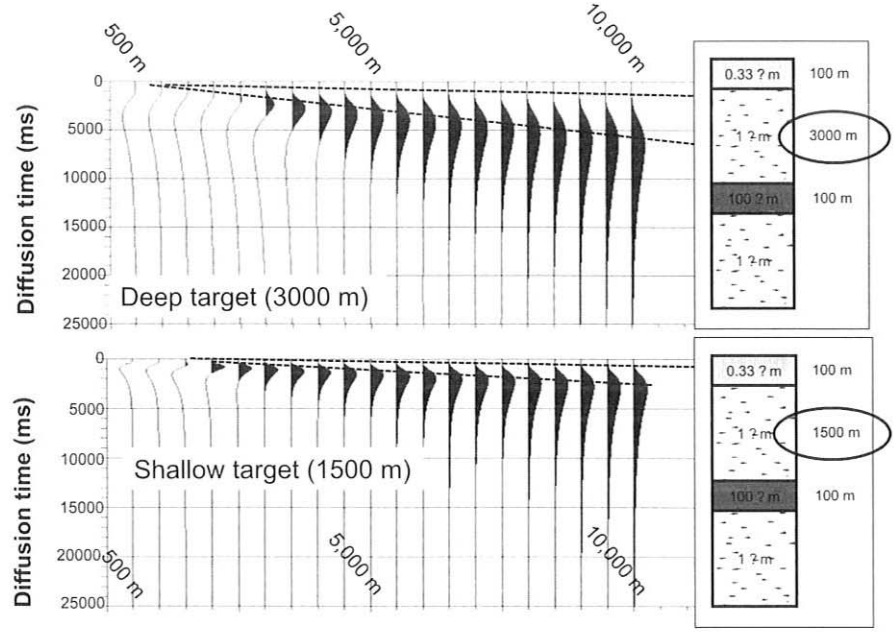

Fig. 7.6 Common-source gathers for the impulse response for an inline electric field marine CSEM setup for different reservoir depths. The traces represent different offsets between source and receiver; displayed are measured voltages. All traces are displayed trace normalized. The Earth model has an oil reservoir at 3000 m or 1500 m depth below the seafloor, respectively. Comparing both gathers shows that a response from a deep target arrives later (After Allegar et al. 2008)

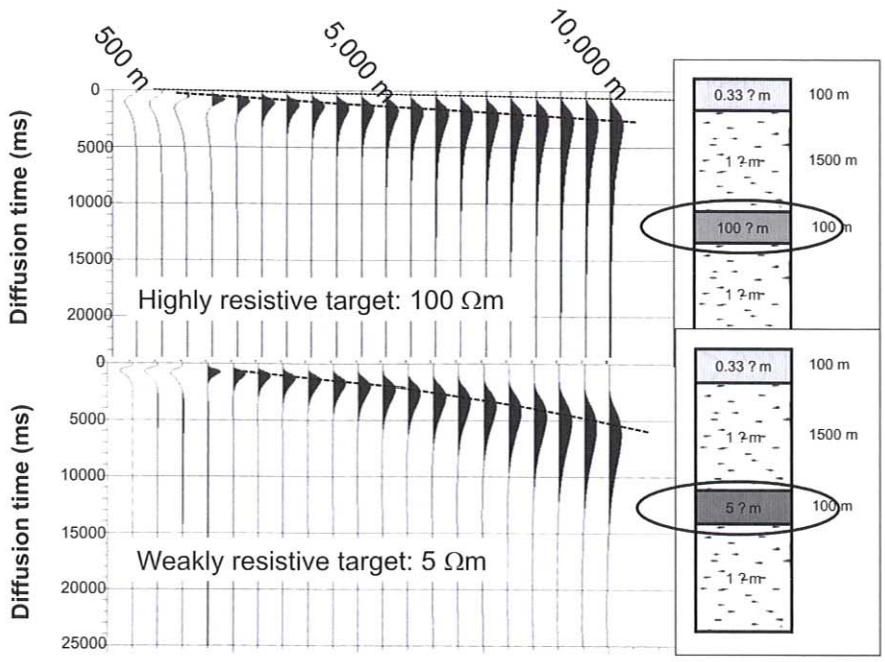

Fig. 7.7 Common-source gathers for the impulse response of an inline electric field marine tCSEM setup. The traces represent different offsets between source and receiver; displayed are measured voltages. All traces are displayed trace normalized. The Earth model has an oil reservoir at 1500 m depth below the sea floor with different resistivities. Comparing gathers shows that for a less resistive (brine saturated) reservoir the signals arrive later and are "smeared" more

with deep source and receivers, when the system only sees the ocean wave. The bottom of the figure shows the case when the system is close to the air-water interface and so also sees the airwave. Note that in this case the airwave gets less attenuated than the ocean wave.

Figure 7.5 shows the gather for the model shown with shallow water layer, with reservoir at 1500 m depth. At the top, all wave components are included, and at the bottom only the reservoir response is shown. This can be obtained by subtraction of the other components, based on the models run without a reservoir. This is easily done with modeled data. For field data, one usually requires a reference measurement over similar geology. This reference data set is then subtracted and the remainder contains the difference between reservoir and non-reservoir model. In the figure (top) we see that at far offsets, the reservoir response arrives after the airwave, but before the sediment and ocean wave, both of which are conductors and maintain induction currents flow longer.

Figure 7.6 displays offset gathers for varying depths to the reservoir, and illustrates that for greater depth the reservoir signal arrives later and gets dispersed more. These behaviors are expected from time domain electromagnetic signals.

Figure 7.7 shows the case of a strongly resistive versus a weakly resistive reservoir. In the case of a weakly resistive reservoir (bottom) the signals flow longer in the reservoir and consequently arrive later. Here, the dispersion at larger offset is even more visible, since the signal from less resistive targets arrives later.

It is often asked about the differences between time and frequency domain surveys. Both Weiss (2007) and Davydycheva (Davydycheva and Rykhlinski 2009) prefer time domain for shallow water applications. Of course for identical survey geometry and timing, data recorded in time domain can always be Fourier-transformed to the frequency domain for analysis. But, as the terms are used in the EM community, they imply *different* survey geometry and/or timing, so the data sets are NOT Fourier-equivalent. Perhaps better terms would be "continuous-source" for fCSEM, and "transient-source" for tCSEM^{TM}, but it is probably too late to change the conventional usage. In frequency domain, the data samples the entire volume between transmitter and receiver, as the secondary field is

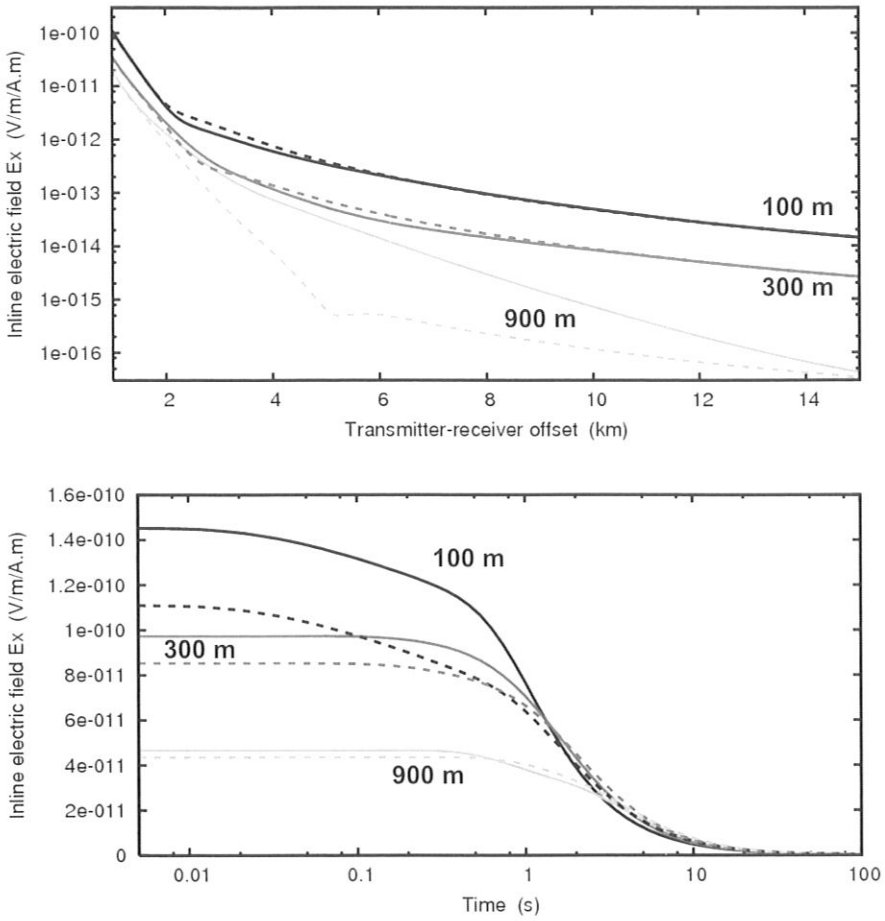

Fig. 7.8 Anomalous response for shallow and deep water for time and frequency domain, with (*solid lines*) and without (*dashed lines*) a resistive reservoir. The *top curves* show the frequency domain response averaged over all times, and the *bottom curves* show the time domain response for a 3 km receiver-to-transmitter offset

recorded in the presence of a continuous primary field. In time domain at each time step the energy is concentrated in a central diffusion volume and the corresponding data are thus more sensitive to the response from within that volume only. So looking at the underneath complex structure is obviously easier with focused EM than with the geometric averaging of fCSEM. While fCSEM has to measure a small secondary response in the presence of a large primary field, in the absence of a primary field, time domain CSEM can amplify the signal. But time domain CSEM is seriously hindered in the application of simple signal-to-noise ratio enhancement; e.g. when the boat is moving, vertical stacking can only be applied to a limited extent. *It seems that both should be used in complementary fashion: fCSEM to outline the resistors and time domain to focus on specific small volumes that are too detailed for fCSEM (like sub-salt targets).*

Figure 7.8 shows the comparison between deep and shallow water anomalies for time and frequency domain surveys. In both the cases, we plot normalized inline electric field magnitudes for 1-D models with 3 different water depths (100, 300, and 900 m), both with (solid lines) and without (dashed lines) a reservoir (100 m thick, 1000 m deep in a 0.7 ohm-m background). The top curves are the frequency domain curves and the bottom curves are the time domain curves. For the time domain plot, we selected offset of 3 km, which is not a significant parameter (Spies 1989). Comparing both plots it can be clearly seen that, for frequency domain measurements, the largest anomalous response can be obtained for deep water. For time domain, the anomalous response is largest for shallow water. The present state of instrumentation favors fCSEM but it will only be a matter of time before time domain will reach similar level for shallow water applications.

7.3 Data Processing and Interpretation

Marine time domain data is recorded using ocean bottom nodes or ocean bottom cables. Nodes are autonomous acquisition systems with multiple electric and magnetic field component sensors that are dropped from the surface onto the ocean floor. As the landing orientation is not known, the data needs to be rotated to a known orientation. Ocean bottom cables (OBC) are carefully laid on the sea floor and orientation is measured with various orientation devices. Nodes are commonly spaced at about 1 km (in special applications as closely as 500 m), while OBCs have 50 or 100 m sensor spacing. The data is usually recorded in a proprietary instrument format, and then converted to SEG D format or SEG Y format, which is the standard for data processing exchange.

The first step in data processing (Fig. 7.9) is the header completion with all survey parameters, navigation parameters, header check, and merging with the source records. The source-to-receiver timing synchronization is a key issue, in time domain as everything is based on the correct timing. While today's electronics drift very slowly, they still exhibit sudden clock jumps, which need to be corrected in data processing.

Next, the data is processed pre-stack to get the optimum signal-to-noise ratios. While today's computers are much faster, most of the filters were already invented decades ago and are described in (Strack et al. 1989, Strack 1992, Strack and Vozoff 1996). Today's improvements in digital processing techniques are mostly restricted to handling more data automatically or graphically.

After the pre-stack processing the stacking or vertical averaging follows. Consecutive shots from a moving boat are not really experimental replicates, but the limited subsurface resolution allows us to stack the data between 0.9 and 1.1 times each nominal offset from the receiver. As the boat moves at about 2 knots, this usually is not more than 4–8 shots in each stack. Thus it is very important to have a strong clean and repeatable source. However, high-frequency deviations from the ideal step source are not important, as they do not survive the propagation down to the target level and back; all the important data are of low frequency. After stacking we can process the data further and convert it into apparent resistivities for input in various interpretation schemes.

Figure 7.10 shows examples of raw data traces. In both the cases, a more conservative bi-polar source

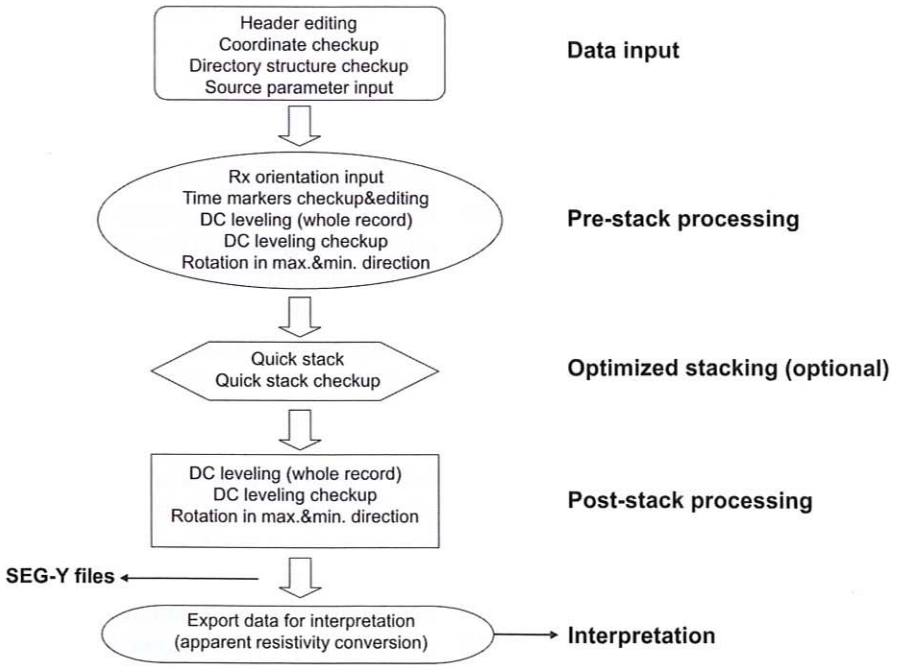

Fig. 7.9 Flow diagram of the various processing steps

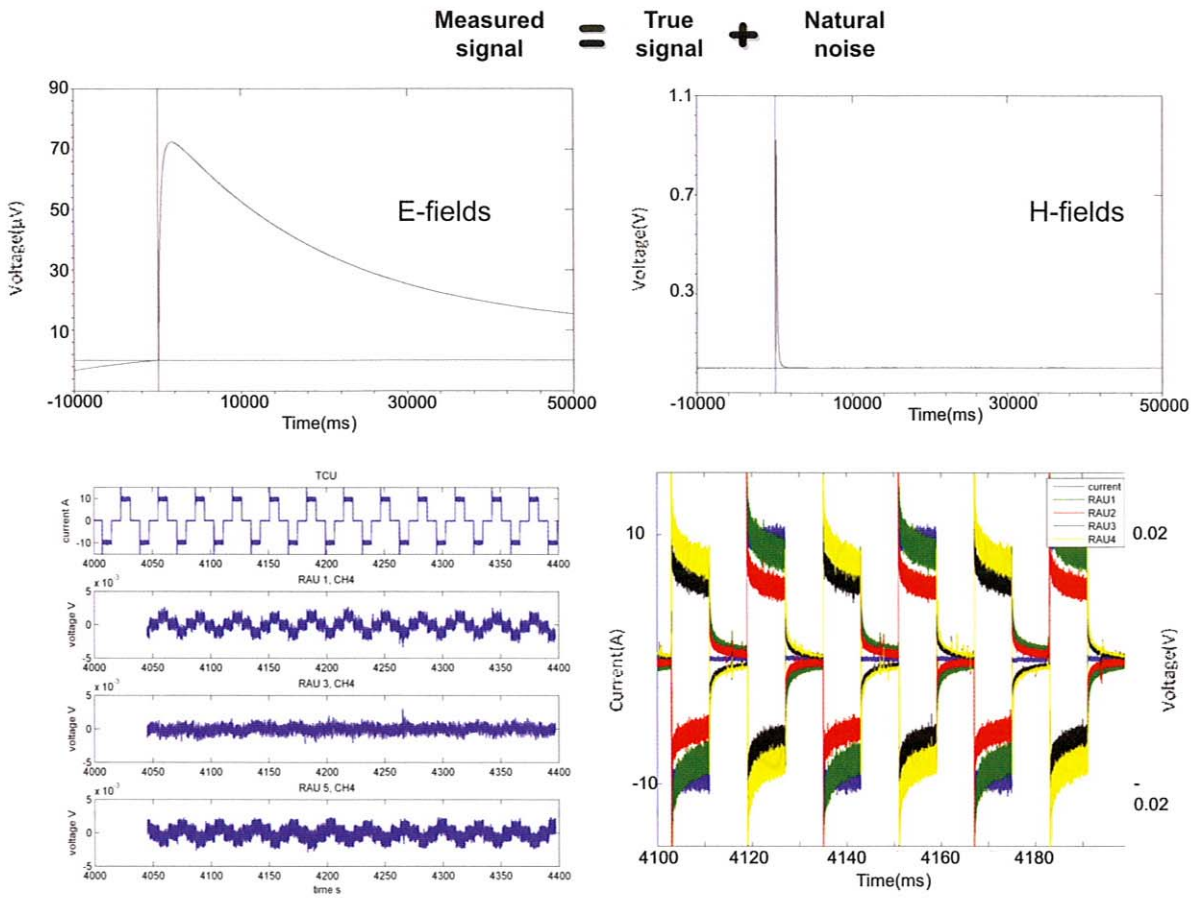

Fig. 7.10 Raw data example traces for a nodal and cabled time domain EM system

waveform (shown in the left-middle) was used. The top of the diagram shows electric and magnetic fields recorded with a nodal system. Both recordings are of good quality. The bottom two diagrams are recorded in very shallow water with a marine cable system under noise conditions. You can clearly see in both electric and magnetic field signals that the responses caused by the source switching. For the upper curves, the time between source switching was 50 s and for the lower curves it was 10 s. The lower curves show the data recorded with different remote acquisition units at different offsets (which accounts for the various amplitudes), in different colors.

Figure 7.11 shows two vector data sets, the top one is un-rotated in raw form (x,y), and the bottom one is rotated into the source-receiver direction (EI, HI) and the cross-line direction (EC, HC). This is the first step in processing to ensure that the amplitudes are treated in an undistorted fashion.

In the next step, one addresses various noise issues in the data. In particular, timing verification is important, because the skipped time marks can distort the processed data. After DC-leveling and filtering, the signal is smoothed with a time-variant smoothing filter as described in Strack et al. (1989) and Strack (1992). The results are shown in Fig. 7.12, whereas on the left is the original transient and on the right is the smoothed version. The smoothed data is then usually averaged (robust stacked) to further improve the signal-to-noise ratios. For normal marine acquisition, the processing stops here and the output data, filed either as EDI or as SEGY. This is usually the interface for interpretation.

Still there is one more still a step left to correct the data. This step may be necessary since, for the reasons of operational efficiency, the delay time between shots may not be sufficient to permit the charge set up from previous shots to completely dissipate. We call this incomplete relaxation as "run-on", and correct for

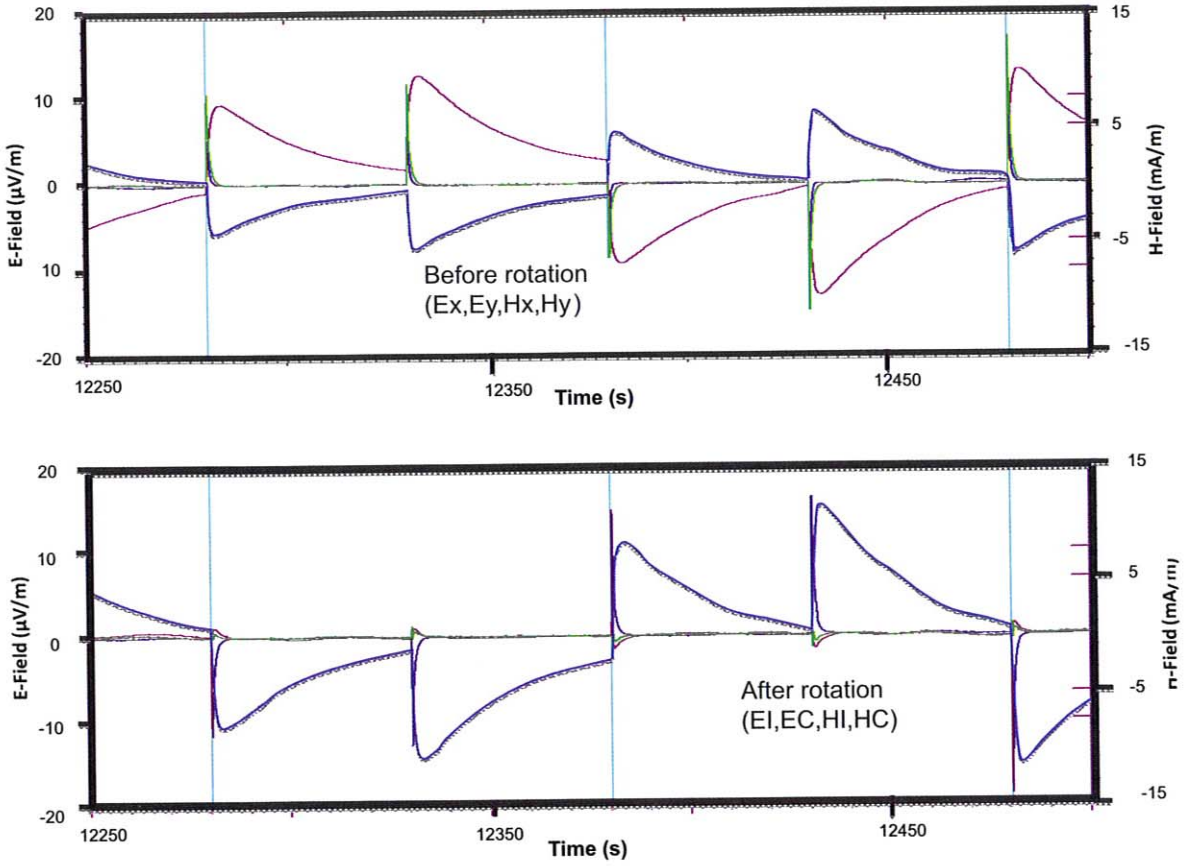

Fig. 7.11 Raw data sample traces (un-rotated) and rotated in the direction of the source dipole

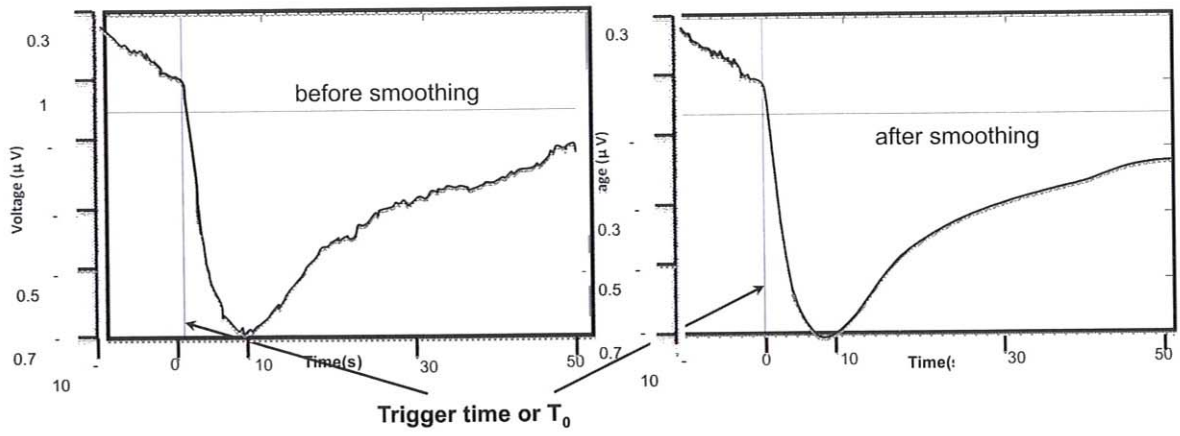

Fig. 7.12 Marine time domain EM sample data: On the left is a raw transient and on the right its smoothed equivalent

it iteratively so that each shot may be analyzed as if no other shots were interfering (Stoyer and Strack 2008).

Interpretation flow diagram using graphical representation is shown in Fig. 7.13. It shows that multiple components are the input into the inversion. Usually with two redundant electric field components, multi-components can be used in a joint or cooperative inversion mode.

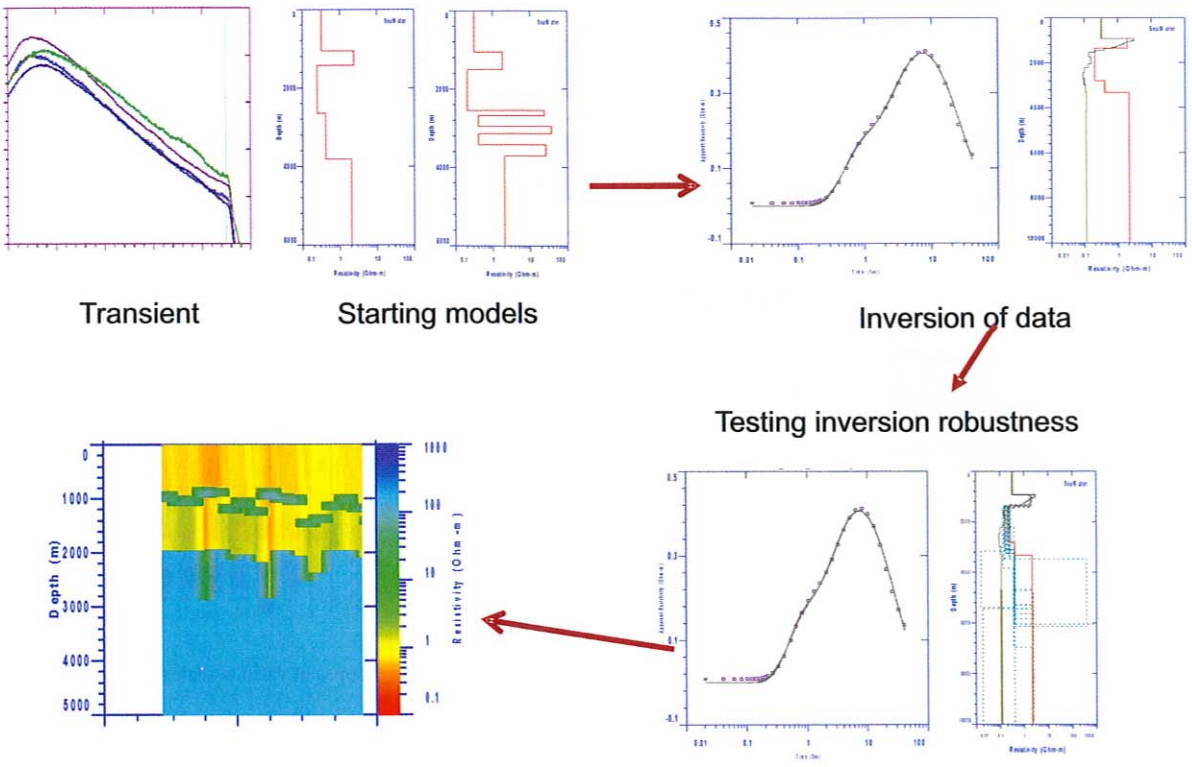

Fig. 7.13 Interpretation flow diagram for marine time domain data

When carrying out the interpretation, two starting models are often used: one for the case with reservoir and the other without. Both the cases are usually tested. When this reservoir/no-reservoir approach is not using, one would use an anisotropic model to ensure the best resistivity structure. When inverting the data, usually various inversion algorithms are compared. In the Fig. 7.13, on the upper right hand side, we compared a layered model with smooth model. When a satisfactory match has been found between the data and results, the final inversion model are compared as shown in this diagram.

When the match is satisfactory, the reliability of the result needs to be estimated to get the right input for the risk analysis. This estimation can be done in various ways. The most reliable method is to use the statistics of the inversion as described by Raiche et al. (1985) or Strack (1992). Other methods using equivalence analysis are also possible, though it is not always driven by data sensitivity. An example of an equivalence analysis is shown in Fig. 7.13 at the bottom right. Once the interpreter is satisfied with the inversion quality, color sections can be seen as shown on the bottom left side of the figure.

7.4 Anisotropy

The biggest factor influencing the surface resistivity measurements is electrical anisotropy. When using electric field measurements, anisotropy caused by layering is "transverse isotropy", i.e. with vertical resistivity different from horizontal resistivity (but the bulk resistivities being the same in horizontal/azimuthal directions). This effect was studied earlier also (Harthill 1968, Strack 1992). It is well known that when using an electric dipole source with primary horizontal diffusion paths, we measure the vertical resistivity with electric fields. Unfortunately, until the advent of tensor induction, this could not be calibrated with normal induction logs in vertical wells. Today i.e. more than 10 years after the 3D induction tool became available, we have enough calibration measurements to make reasonable estimates of the effect.

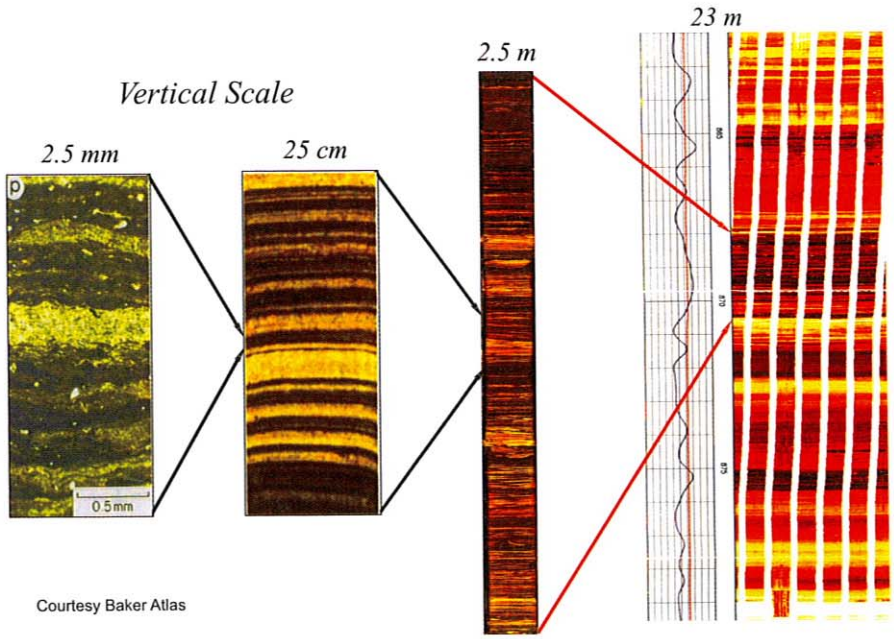

Fig. 7.14 Example of anisotropic images from image logs, core scans and electron microscopes at various scales

Figure 7.14 shows an example for the presence of anisotropy at all scales. On the right side of the figure, images from electrical logs are shown. On the left side of the figure, we see core images of various scales with electron-microscope images on the for left of the figure The light colors are the sand and the dark colors are the shales. We can clearly see thin laminations everywhere that result in electrical anisotropy. Normal anisotropy values (vertical resistivity/horizontal resistivity) are between 1.2 and 1.4 in sedimentary basin but they can go as high as 10.

A factor to be considered is azimuthal anisotropy and its interaction with dipole field from the transmitter. Hördt (1992) studied this for Long Offset Transient Electromagnetic (LOTEM) measurements and determined that there was an optimum azimuthal orientation of the source dipole, where one or the other measured component would be preferred (Fig. 7.15). Another interesting result from Hördt is that this optimum area is discerned only 2–3 times the transmitter dipole length away from the source, which confirms that TEM measurements can work with much closer offsets than frequency domain soundings. So far, from our experience we found that many elements from land measurements translate directly to the marine environment, and we assume that this is the case here also.

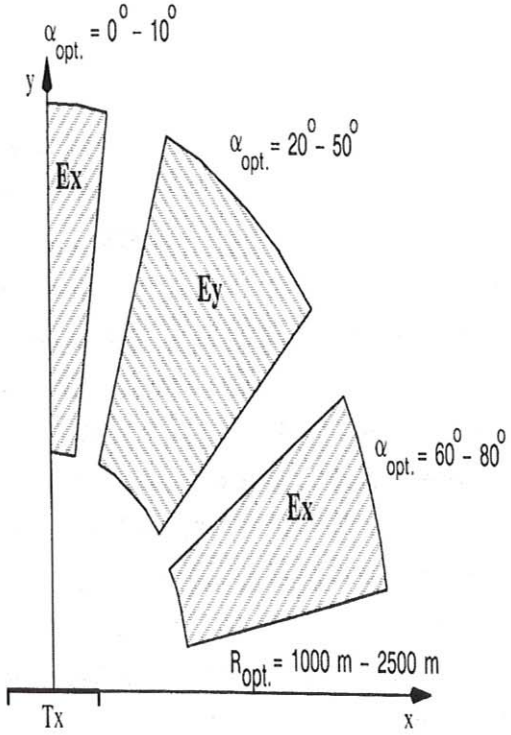

Fig. 7.15 Azimuthal distribution of the optimum component for surface measurements using electric fields and a Lotem setup (after Hördt 1992)

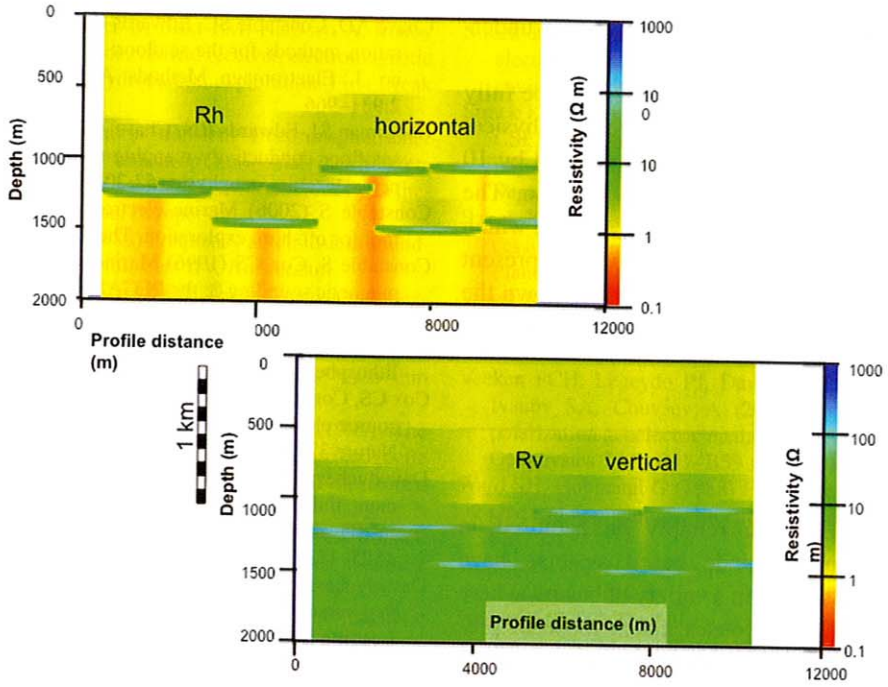

Fig. 7.16 Examples of two inverted stitched 1-D section using vertical and horizontal resistivities in a joint inversion mode

Figure 7.16 shows an example of an anisotropic inversion, with both vertical and horizontal resistivity sections. Note that horizontal resistivities often have more artifacts (vertical stripes), which are reduced in vertical resistivity inversion. Sub articificials may be a result of style of inversion. For example, in "stitched 1D" (i.e. independent 1D inversions repeated along a 2D profile, with varying results simply stitched together, despite existence of inconsistency. This procedure can work well with slow lateral variation and does not work well when the subsurface varies substantially on the scale of the source-receiver offset.

7.5 The Future and Pitfalls

The past twenty years have shown great progress in electrical geophysics especially in marine environment. With the advent of new logging tools, one can calibrate surface measurements and understand the anisotropy and production efficiently. Anisotropy is still the biggest pitfall, because its influence on resistivity measurements sometimes as high as 50%. Another factor influencing the EM signal is the induced Polarization. It is commonly observed and interpreted mainly in Russia and China. We have seen it in marine data but have been able to interpret the data using normal electromagnetic models without polarization effects.

A strong factor often ignored is the physical complexity of the subsurface resistivity distribution, not well imaged when using a system with several kilometers of source-to-receiver offset. It is well known that the Earth is rarely 1-dimensional. Thus shorter offsets are preferred to longer offsets, in order to resolve the subsurface complexity.

Predicting the future of marine EM is more complex. We have to make assumptions to do the right extrapolation. In 5 years period we assume:

- Marine Electromagnetics is in use (at least occasionally) by most oil companies, through their contractors.
- Reservoir monitoring will be the key focus of oil companies.
- Integration with seismic/geology will bring the value of EM to the forefront.
- Marine measurements will be done much denser with lower unit cost.
- Land measurements will still have limited applications unless integrated with seismic data acquisition.

- The integration value of EM will be better understood.

In summary, marine, electromagnetics will be fully complementary and integrated with other geophysical methods. The unit cost will have to be reduced by 10 fold in order to fit in a more routine scenario. The strongest market will be the monitoring market, which will require a change of business model for present service companies, as the oil companies will own the installations. Monitoring will include land and marine systems.

7.6 Conclusions

Time domain CSEM can reliably be acquired in a marine environment. Node based systems have acquired multiple data sets in a variety of basins, where the recorded transient responses match those of pre-survey models. We have adapted the methods from onshore environment to offshore and shown that the results are very similar. We also tested the next generation technology, a cabled version of the system and so far the signal behaves as anticipated. Time domain EM is optimum in shallow waters, but should really be used in a complementary fashion to frequency domain and marine magnetotellurics. Developments with a cabled system and initial functionality tests are very promising, in particular with respect to minimizing transmitter-to-receiver offset and resolving anisotropy.

Acknowledgements We thank KMS Technologies for permission to publish this material. Throughout the development of this work we received support from EMGS and BP and are grateful for that. Many colleagues have contributed to this work, a very special thanks to them. In particular, N. Allegar, I. Loehken, and Y. Martinez were very supportive in getting the task accomplished. A. A. Aziz and K. Vozoff were of great assistance in preparing the manuscript.

References

Avdeeva A, Commer M, Newman G (2007) Hydrocarbon reservoir detectability study for marine CSEM methods: time domain versus frequency domain: 78th international annual meeting. Soc Exploration Geophysicists, Expanded Abstr 26:628–632

Allegar NA, Strack KM, Mittet R, Petrov A (2008) Marine time domain CSEM – the first two years of experience. In: 70th conference & exhibition, European Association expanded abstract vol. Geoscientists & Engineers, Rome, Italy

Chave AD, Constable SC, Edwards RN (1991) Electrical exploration methods for the seafloor: investigation in geophysics no 3. Electromagn Methods Appl GeophysAppl Part B 2:931–966

Cheesman SJ, Edwards RN, Chave AD (1987) On the theory of sea-floor conductivity mapping using transient electromagnetic systems. Geophysics 52:204–217

Constable S (2006) Marine electromagnetic methods—a new tool for offshore exploration. The Leading Edge 25:438–444

Constable S, Cox CS (1996) Marine controlled source electromagnetic sounding 2: the PEGASUS experiment. J Geophys Res 101:5519–5530

Cox CS (1981) On the electrical conductivity of the oceanic lithosphere. Phys Earth Planetary Inter 25:289–300

Cox CS, Constable SC, Chave AD, Webb SC (1986) Controlled-source electromagnetic sounding of the oceanic lithosphere. Nature 320(6057):52–54

Davydycheva S, Druskin V, Habashy T (2003) An efficient finite-difference scheme for electromagnetic logging in 3D anisotropic inhomogeneous media. Geophysics 68: 1525–1536

Davydycheva S, Rykhlinski N (2009) Focused-source EM survey versus time-domain and frequency-domain CSEM. The Leading Edge 28:944–949

Druskin V, Knizhnerman L (1994) Spectral approach to solving three-dimensional Maxwell's diffusion equations in the time and frequency domains. Radio Sci 29(4):937–953

Eadie T (1979) Stratified earth interpretation using standard horizontal loop electromagnetic data. Research in applied geophysics, vol 9. Geophysics Laboratory, University of Toronto, Toronto

Edwards RN, Law LK, Wolfgram PA, Nobes DC, Bone MN, Trigg DF, DeLaurier JM (1985) First results of the MOSES experiment: sea sediment conductivity and thickness determination, Bute Inlet, British Columbia, by magnetometric offshore electrical sounding. Geophysics 50:153–160

Edwards RN (1987) Controlled source electromagnetic mapping of crust. In: James DE (ed) Encyclopedia of geophysics, geomagnetism and paleomagnetism volume. Van Nostrand Reinhold Co. Inc., Stroudsburg, Invited paper, pp 126–139

Edwards RN (1997) On the resource evaluation of marine gas hydrate deposits using the sea-floor transient electric dipole-dipole method. Geophysics 62:63–74

Edwards RN, Yu L (1993) First measurements from a deep-tow transient electromagnetic sounding system. Mar Geophys Res 15:13–26

Eidesmo T, Ellingsrud S, MacGregor LM, Constable S, Sinha MC, Johansen S, Kong FN, Westerdahl H (2002) Sea bed logging (SBL), a new method for remote and direct identification of hydrocarbon filled layers in deep water areas. First Break 20:144–152

Harthill N (1968) The CSM test area for electrical surveying methods. Geophysics 33:675–678

Hohmann GW (1988) Numerical modeling for electromagnetic methods of geophysics. In: Nabighian MN (ed) Electromagnetic methods in applied geophysics. Vol. 1, pp 313–363

Holten T, Flekkøy G, Måløy KJ, Singer B (2009a) Vertical source and receiver CSEM method in time domain. Soc Exploration Geophysicists, Expanded Abstr 28: 749–753

Holten T, Flekkoy G, Singer B, Blixt EM, Hanssen A, Maloy KJ (2009b) Vertical source, vertical receiver, electromagnetic technique for offshore hydrocarbon exploration. First Break 27:89–93

Hördt A (1992) Interpretation transient elektromagnetischer Tiefensondierungen für anisotrop horizontal geschichtete und für dreidimensionale Leitfähigkeitsstrukturen: Ph D thesis, University of Cologne, Europe

Kaufman AA, Keller GV (1983) Frequency and transient soundings. Elsevier Science Publishers BV, Amsterdam

Newman GA, Alumbaugh DL (2000) Three-dimensional magnetotelluric inversion using non-linear conjugate gradients. Geophys J Int 140:410–424

Passalacqua H (1983) Electromagnetic fields due to a thin resistive layer. Geophys Prospecting 31:945–976

Raiche AP, Jupp DLB, Rutter H, Vozoff K (1985) The joint use of coincident loop transient electro-magnetic and Schlumberger sounding to resolve layered structures. Geophysics 50:1618–1627

Sinha MC, Patel PD, Unsworth MJ, Owen TRE, MacCormack MGR (1990) An active source electromagnetic sounding system for marine use. Mar Geophys Res 12:29–68

Spies BR (1989) Depth of investigation in electromagnetic sounding methods. Geophysics 54:872–888

Stoyer CH, Strack KM (2008) Method of acquiring and interpreting electromagnetic measurements. US Patent 07356411

Strack KM (1992 and 1999) Exploration with deep transient electromagnetics – introduction and indexes. Elsevier Science Publishers BV, Amsterdam

Strack KM, Petrov AA (2007) Marine time domain controlled source electromagnetics (tCSEM^{TM}): another way to illuminate marine, reservoirs. In: Proceedings of the 8th China international geo-electromagnetic workshop, Jingzhou, China, paper 3, pp 9–14

Strack KM, Vozoff K (1996) Integrating long-offset transient electromagnetics (LOTEM) with seismics in an exploration environment. Geophys Prospecting 44:99–101

Strack KM, Allegar N, Ellingsrud S (2008) Marine time domain CSEM: an emerging technology. Society exploration geophysicists. In: Annual meeting, extended abstracts, Las Vegas, pp 653–656

Strack KM, Hanstein TH, Eilenz HN (1989) LOTEM data processing for areas with high cultural noise levels. Phys Earth Planetary Inter 53:261–269

Strack KM, Hanstein T, Lebrocq K, Moss DC, Petry H, Vozoff K, Wolfgram PA (1989) Case histories of LOTEM surveys in hydrocarbon prospective areas. First Break 7:467–477

Veeken PCH, Legeydo PJ, Davidenko YA, Kudryavceva EO, Ivanov SA, Chuvaev A (2009) Benefits of the induced polarization geoelectric methods to hydrocarbon exploration. Geophysics 74(2):B47–B59

Ward SH, Hohmann G (1988) Electromagnetic theory for geophysical applications. Electromagn Methods Appl Geophys SEG 1:131–311

Weidelt P (2007) Guided waves in marine CSEM. Geophys J Int 171(1):153–176

Weiss CJ (2007) The fallacy of the "shallow-water problem" in marine CSEM exploration. Geophysics 72(6):A93–A97

Wright D, Ziolkowski A, Hobbs B (2002) Hydrocarbon detection and monitoring with a multicomponent transient electromagnetic (MTEM) survey. Leading Edge 60: 481–500

Ziolkowski A, Hall G, Wright D, Carson R, Peppe O, Tooth D, Mackay J, Chorley P (2006) Shallow marine test of MTEM method. 76th Annual International Meeting. Soc Exploration Geophysicists, Expanded Abstr 25:729–734

KMS Technologies – KJT Enterprises, Inc.

6420 Richmond Ave., Suite 610
Houston, Texas 77057, USA
Tel: +1 713.532.8144
Fax: +1 832.204.8418

www.KMSTechnologies.com